

Transition Multipolarities in ^{143}Pr and ^{141}Pr

W. GELLETTY,* J. S. GEIGER, AND R. L. GRAHAM

Chalk River Nuclear Laboratories, Atomic Energy of Canada Limited, Chalk River, Ontario, Canada

(Received 30 October 1967)

Measurements of L -shell internal conversion line intensity ratios are reported for the 57.37- and 293.3-keV transitions in ^{143}Pr and for the 145.43-keV transition in ^{141}Pr . The measurements were made, using a 100-cm-radius iron-free $\pi\sqrt{2}$ double-focusing β spectrometer at a resolution setting of 0.05% in momentum. Comparison with theoretical L -shell internal conversion coefficient ratios gives multipolarities for the 57.37-keV γ ray of $(99.85 \pm 0.03)\% M1 + (0.15 \mp 0.03)\% E2$ and for the 293.3-keV γ ray of $(63 \pm 4)\% M1 + (37 \mp 4)\% E2$. The measured K -conversion coefficient for the 57.37-keV transition is 5.64 ± 0.34 . Analysis of the ^{143}Pr results in combination with the 293- and 57-keV γ - γ angular correlation results of other experimenters indicates a $\frac{5}{2}+$ assignment for the 57.37-keV level and a $\frac{3}{2}+$ assignment for the 350.7-keV level in ^{143}Pr . The multipolarity of the 145.43-keV transition in ^{141}Pr is $(99.58 \pm 0.08)\% M1 + (0.42 \mp 0.08)\% E2$.

I. INTRODUCTION

THE main features of the ^{143}Ce decay scheme were established more than a decade ago by Martin *et al.*,¹ without any definite proposals for spin and parity assignments for the states in ^{143}Pr . In 1962, Rao and Hans² reported a study of conversion coefficients and the 293- and 57-keV angular correlation. Assuming that the ground state of ^{143}Pr had spin parity $\frac{5}{2}+$, they deduced that the 57- and 351-keV levels must have assignments of $\frac{7}{2}+$ and $\frac{3}{2}+$, respectively. However, the atomic beam measurement of Budick *et al.*,³ established that ^{143}Pr had a ground-state spin of $\frac{7}{2}$. Measurements of the L -subshell internal conversion ratios by Graham *et al.*⁴ showed that the 57.37-keV transition was $M1 + \leq 0.3\% E2$ and that the 293.3-keV transition was $(66 \pm 16)\% M1 + (34 \pm 16)\% E2$. With these restrictions on multipolarity admixtures they reanalyzed the angular correlation data of Rao and Hans¹ and concluded that the 57-keV level assignment was $\frac{5}{2}+$ and that the spin of the 351-keV level could be either $\frac{3}{2}$ or $\frac{7}{2}$.

During the next three years there were several investigations, each of which favored one or the other choice of spin for the 351-keV level. In 1964 Simons *et al.*⁵ reported measurements of the 293- and 57-keV, 665- and 57-keV, and 230- and 490-keV γ - γ angular correlations. They found a somewhat smaller anisotropy for the 293- and 57-keV γ - γ correlation ($A_2 = 0.106 \pm 0.010$)⁵ than that reported earlier ($A_2 = 0.132 \pm 0.019$).² Making the assumption that the 57-keV transition was pure $M1$, they concluded that the 351-keV level must be $\frac{7}{2}+$, the 490-keV level $\frac{5}{2}$, $\frac{7}{2}$, or $\frac{9}{2}$, and the 725-keV level $\frac{3}{2}$ or $\frac{7}{2}$. The same correlations were also studied by

Mancuso *et al.*,⁶ and they too concluded that the 351-keV level assignment was $\frac{7}{2}+$. Four γ - γ correlations were studied by Gopinathan.⁷ However, he concluded that $\frac{3}{2}+$ was the most probable assignment for the 351-keV level.

By 1966, it was clear that studies of the γ - γ directional correlations could not lead to an unambiguous spin for the 351-keV level, although there was no doubt as to the spins of the ground state and the first excited state at 57 keV. This is often the case when attempting to interpret γ - γ correlation data. Independent and accurate knowledge of some or all of the γ -ray multipolarities is frequently needed before one can interpret the measured correlations unambiguously to yield nuclear level spins. This spin ambiguity in ^{143}Pr appeared to have been removed by the careful measurements of five γ - γ correlations by Sunyar and Thieberger.⁸ These led to spin-parity assignments of $\frac{5}{2}+$, $\frac{3}{2}+$, $\frac{5}{2}+$, and $\frac{3}{2}+$ for the 57-, 351-, 491-, and 722-keV states. An interesting corollary of the analysis of their data was the condition that the 57-keV transition must be pure $M1$ with $< 0.006\% E2$. This condition was consistent with the earlier published limit of $\leq 0.3\%$ ⁴ but not with unpublished data then available at our laboratory.

In this paper we report new and more accurate values for the $E2$ admixtures in the 57- and 293-keV transitions in ^{143}Pr which have been obtained from measurements of the L -subshell internal conversion line intensity ratios. These indicate an $E2$ admixture of $(0.15 \pm 0.03)\%$ in the 57.37-keV transition, in disagreement with the conclusion of Sunyar and Thieberger.⁸ This disagreement could arise from (a) dynamic nuclear penetration effects in the internal conversion process which are not included in the tabulated $M1$ coefficients or (b) attenuation effects in the 293- and 57-keV γ - γ directional correlation which have not been detected. As a test for the first of these possibilities we have measured

* Present address: Brookhaven National Laboratory, Upton, N. Y.

¹ D. W. Martin, M. K. Brice, J. M. Cork, and S. B. Burson, *Phys. Rev.* **101**, 182 (1956).

² G. N. Rao and H. S. Hans, *Nucl. Phys.* **41**, 511 (1963).

³ B. Budick, W. M. Doyle, R. Marrus, and W. A. Nierenberg, *Bull. Am. Phys. Soc.* **7**, 477 (1962); B. Budick, I. Maleh, and R. Marrus, *Phys. Rev.* **135**, B1281 (1964).

⁴ R. L. Graham, J. M. Hollander, and P. Kleinheinz, *Nucl. Phys.* **49**, 641 (1963).

⁵ L. Simons, A. Anttila, and S. Bergström, *Soc. Sci. Fennica, Commentationes Phys.-Math.* **30**, No. 3 (1964).

⁶ R. V. Mancuso, J. P. Roalsvig, and R. G. Arns, *Phys. Rev.* **140**, B525 (1965).

⁷ K. P. Gopinathan, *Phys. Rev.* **139**, B1467 (1965).

⁸ A. W. Sunyar and P. Thieberger, *Bull. Am. Phys. Soc.* **11**, 407 (1966).

the absolute K internal conversion coefficient of the 57.37-keV transition. Our experimental value is in reasonable agreement with the theoretical values of Rose⁹ and of Sliv and Band,¹⁰ and does not support the hypothesis of anomalous conversion. Sunyar and Thieberger have studied the time dependence of the 293- and 57-keV γ - γ directional correlation in a search for previously undetected attenuation. This search has proven successful¹¹; by extrapolating their results to zero time they obtain a larger A_2 coefficient for this correlation than any previously reported. The combined set of new data is reexamined here in some detail. The most probable spins are $\frac{5}{2}$ for the 57-keV level and $\frac{3}{2}$ for the 351-keV level.

A brief account of these ^{143}Pr measurements was presented at the meeting of the American Physical Society held in New York in January, 1967 (Ref. 12).

We include in this paper a determination of the multipolarity of the 145.43-keV γ transition ($\frac{7}{2}^+ \rightarrow \frac{5}{2}^+$) in ^{141}Pr based on its L -subshell conversion-line intensity ratios.

II. EXPERIMENTAL TECHNIQUES

The internal conversion electron spectra were measured using the Chalk River iron-free $\pi\sqrt{2}$ β -ray spectrometer.¹³ The electron detector was a flow-type proportional counter which could be fitted with different side-entrance windows. When studying the L lines of the 57-keV transition a thin, $\sim 100\text{-}\mu\text{g}/\text{cm}^2$ VYNS¹⁸ plastic window was used; the counter was operated with methane gas at an absolute pressure of 10 cm Hg and a nickel grid of 85% open area was used to support the window. For studies of the other, more energetic, transitions the counter window was an unsupported Mylar film of $\sim 1\text{ mg}/\text{cm}^2$ and the filling was methane gas at atmospheric pressure.

The ^{143}Ce sources were prepared from Ce_2O_3 enriched to 92.7% in ^{142}Ce which was irradiated to saturation activity in a neutron flux of $2 \times 10^{14}\text{ cm}^{-2}\text{ sec}^{-1}$. The specific activity of this material, only $\sim 20\text{ Ci/g}$, was a limiting factor in this study. To achieve good resolution one must keep the source thickness and source dimensions within well defined limits. To circumvent this limitation on source strength we have used multiple-element sources in the arrangement described by Bergkvist.¹⁴ This permitted us to achieve an order of

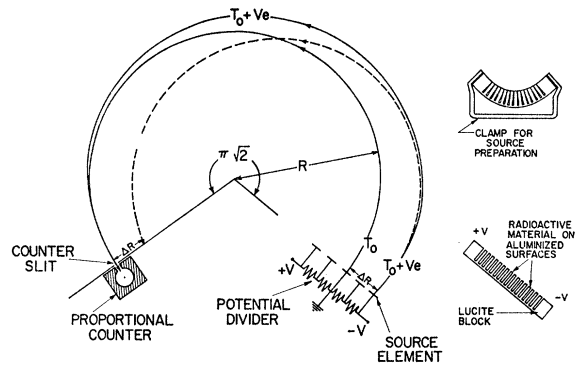


FIG. 1. Schematic diagram illustrating the principle of the multistrip source technique of Bergkvist [Ref. 14]. Thirty individual strip sources 0.5 mm wide by 20 mm high were used (only five are shown here). When the relative potentials are correctly adjusted (see text for details), conversion electrons of initial energy T_0 from all elements are brought to focus at the counter slit. With this technique one can utilize a source area of $15 \times 20\text{ mm}^2$ with the resolution appropriate to a source area of $0.5 \times 20\text{ mm}^2$, thus greatly improving the luminosity.

magnitude higher counting rate than could have been realized with a single-element source.

The principle of the Bergkvist technique can be understood by referring to Fig. 1. Electric fields are used to accelerate or decelerate electrons emerging from the different source elements in such a way that the focused images from the various sources are brought together at the counter slit on the focal plane. Consider first what happens without electric fields; i.e., all source elements in Fig. 1 are at ground potential. The magnetic field is adjusted to focus electrons of energy T_0 emerging from the central source element at R onto the counter slit, also at radius R . Electrons of energy T_0 emerging from the outer source element at $R + \Delta R$ will come to focus at $R - \Delta R$ at the focal plane since the magnification of $\pi\sqrt{2}$ spectrometers is -1 . If we now apply a negative potential V to the outer source element, the electrons will gain an energy of Ve as they leave the source. The higher energy and hence momentum $B\rho$ causes the electrons to follow orbits with a larger radius of curvature, and hence the image moves out towards the counter slit. In the general case there will be a different voltage V_i on each source element i located at a radial distance Δr_i from the central source element at R . To bring all the images together at the counter slit the voltages V_i must satisfy the relation

$$V_i = -\frac{T_0}{e} \left(1 + \frac{m_0 c^2}{m_0 c^2 + T_0} \right) \frac{\Delta r_i}{4R}, \quad (1)$$

where T_0 is the initial electron kinetic energy in keV, e is the electron charge, and $m_0 c^2$ is the rest mass energy of the electron, i.e., 511 keV.

Multistrip ^{143}Ce sources were prepared as follows. The source backing was made from a Lucite block 3 cm wide by 2 cm high and 0.5 cm thick. Thirty-one vertical grooves were machined in the surface to define 30 strips

⁹ M. E. Rose, *Internal Conversion Coefficients* (North-Holland Publishing Co., Amsterdam, 1958).

¹⁰ L. A. Sliv and I. M. Band, *Coefficients of Internal Conversion of Gamma Radiation* (USSR Academy of Sciences, Moscow-Leningrad, 1956), Part I: K Shell, Part II: L Shell; also in α -, β -, and γ -ray Spectroscopy, edited by K. Siegbahn (North-Holland Publishing Co., Amsterdam, 1966), p. 1639.

¹¹ A. W. Sunyar and P. Thieberger (private communication).

¹² W. Gelletly, J. S. Geiger, and R. L. Graham, *Bull. Am. Phys. Soc.* 12, 55 (1967).

¹³ R. L. Graham, G. T. Ewan, and J. S. Geiger, *Nucl. Instr. Methods* 9, 245 (1960).

¹⁴ K. E. Bergkvist, *Arkiv. Fysik* 27, 383 (1964).

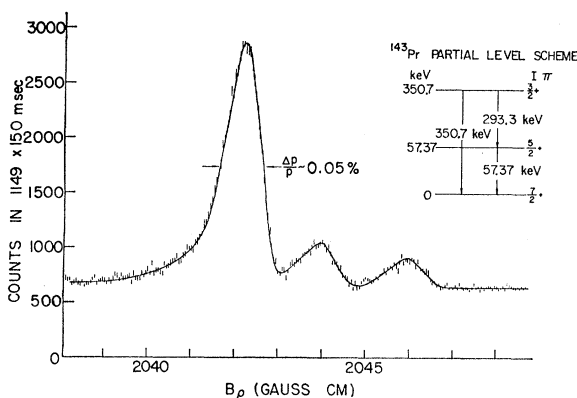


FIG. 2. Spectrum of the L -conversion lines of the 293.3-keV transition in ^{143}Pr .

0.5 mm wide separated by gaps of 0.35 mm. An evaporator was used to coat the outer surfaces of the 30 20 mm \times 0.5 mm strips with an electrically conducting layer of aluminum. The ^{143}Ce activity was deposited on the 30 aluminized surfaces of these strips by sublimation in vacuum from a boat-shaped tantalum filament. When mounted in the β spectrometer the insulated source elements were electrically connected to taps on a potential divider as indicated in Fig. 1. Separate positive and negative regulated voltage supplies were used. In order to satisfy Eq. (1) rigorously, the voltages should be continuously adjusted as the conversion electron spectrum is scanned. However, in each of the scans reported here the range of energy covered ΔT was small compared to T_0 , and so fixed potentials were chosen to satisfy Eq. (1) near the midpoint of the scanned region.

A rapid-scan counting technique was employed in these studies in order to minimize the effects of variations in background counting rate on the observed spectrum. As has been noted earlier¹³ the atmosphere near the β -spectrometer building is sometimes polluted with ^{41}Ar coming from the reactor ventilating stacks. This contaminant has a half-life of 1.8 h and emits a γ ray of 1.29 MeV. Under unfavorable atmospheric conditions we observe an increase in detector background rate of up to ~ 100 counts/min which can change significantly in intensity every few minutes. When scanning the β spectrum by conventional methods, i.e., point-by-point with counting periods of 10 to 40 sec per point, these fluctuations can introduce spurious "lines" in the spectra. To circumvent this difficulty in the present work we have scanned over a 400-point region in 80 sec and achieved good counting statistics by repeating the scan many times. This averages the background fluctuations quite uniformly over all points. The basic features of the rapid-scan technique were first described by Seltzer and Hager.¹⁵ The data

¹⁵ E. Seltzer and R. Hager, in *Internal Conversion Processes*, edited by J. H. Hamilton (Academic Press Inc., New York, 1966).

for each point in the spectrum were stored in separate channels of the memory of a 400-channel analyzer operated in the multiscale mode. The channel address was incremented every fifth of a second. The β -spectrometer field strength was simultaneously incremented by an electrical link between the channel address register and the current regulator. The analog voltage, normally used for display and plotting, is proportional to channel number. This voltage source generated a current "staircase," $0 \leq \Delta I \leq I_s$, which, when added to the fixed reference current I_0 , caused the spectrometer field setting to sweep the desired region of the spectrum. In the work reported here the range of scan I_s/I_0 was typically only a few percent.

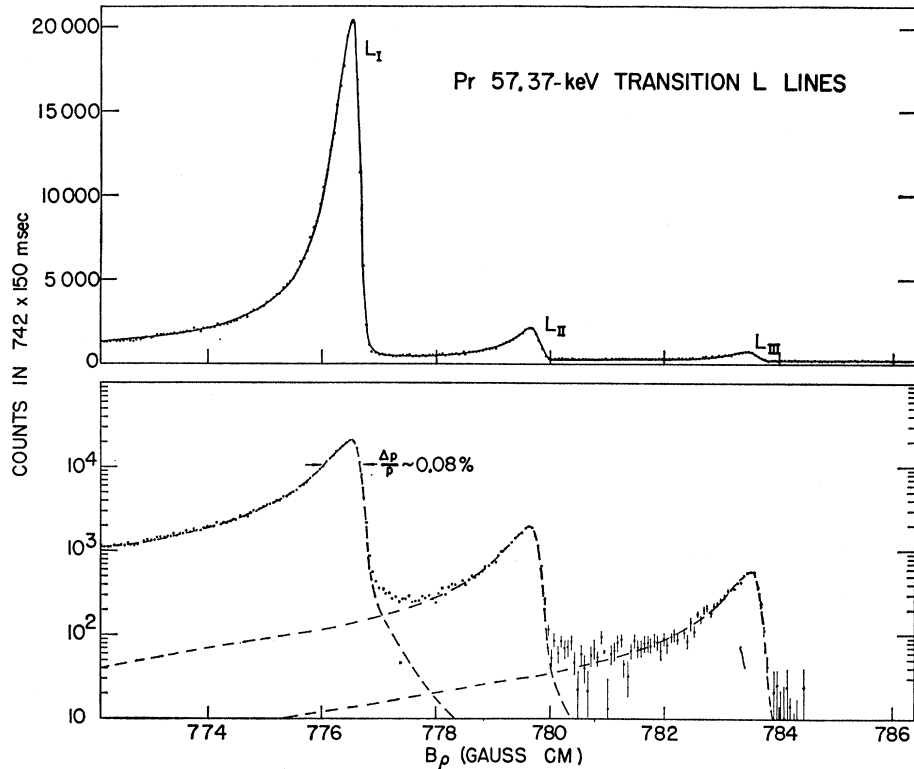
Measurements of the K -conversion coefficient of the 57-keV transition were made using a 30-cm³ Ge(Li) γ -ray detector, a NaI(Tl) scintillation γ counter having a very thin window, a plastic phosphor scintillation β detector, conventional electronics, and a multichannel analyzer. In the initial experiments a pulse-height window was set on the 293-keV peak from the Ge(Li) detector and the coincidence pulse-height spectrum from the thin window NaI(Tl) detector was recorded. A later experiment involved triple coincidences. Coincidences between energetic β rays detected in a plastic phosphor and 293-keV γ rays in the Ge(Li) detector were required to gate pulses from the NaI(Tl) detector; the purpose was to reduce the contribution in the gated NaI(Tl) pulse-height spectrum from 293-keV γ ray and bremsstrahlung coincidences.

III. ^{143}Pr L -SUBSHELL INTENSITY RATIOS

The L -shell internal conversion electron spectrum of the 293-keV transition in ^{143}Pr is shown in Fig. 2. The position of this transition in the ^{143}Pr level sequence is given in the inset. These data were accumulated using a multielement source and the rapid-scan technique for data accumulation. The momentum resolution realized in the measurement was 0.05%. The L internal conversion electron spectrum of the 57-keV transition observed under the same operating conditions is shown in Fig. 3.

The rather poorer momentum resolution realized on these lower-energy lines, 0.084%, and the more pronounced low-energy tails are due to electron energy loss in the finite thickness of source material. The linear plots show the raw data. The net L -conversion line spectrum is obtained from these raw data by subtracting the background contributed by the β continuum and the natural counter background. In these analyses this background has been assumed to be uniform and its value was taken to be the mean count observed in the spectral region above the L_{III} line. The net L line counts for the 57-keV transition are given on a semilogarithmic plot in the lower half of Fig. 3.

FIG. 3. Spectrum of the L -conversion lines of the 57.37-keV transition in ^{143}Pr . The upper part shows the raw data. The lower part shows a logarithmic plot of the net counts after subtracting the contribution from the β continuum and counter background. The peaks are fitted with a common line shape (dashed lines) as discussed in the text.



In our graphical analyses of the net spectra, we have made the working assumption that all three L lines have a common shape on a logarithmic plot. The L_I line has the best statistics and is used as the starting shape except for the high- and low-energy tails, which must first be estimated by graphical extrapolation. One then attempts to fit the experimental data by adjusting the positions and heights of three line shapes. The tail shapes are then readjusted and the fitting procedure is iterated until the sum of the three shapes provides an acceptable fit to the experimental data. The dashed line shapes in Fig. 3 resulted from such a fitting procedure.

This working assumption of a common line shape is not strictly valid; one expects small differences from the following three effects:

(a) The different natural widths of the L_I , L_{II} , and L_{III} atomic states.

(b) The instrumental linewidth $\Delta p/p$ is constant, hence Δp is proportional to momentum and $\Delta p(L_{III}) > \Delta p(L_I)$.

(c) Electron energy losses in the finite thickness of the source layer. These will be proportionally greater for the L_I line than the L_{III} line.

The natural widths of L -shell vacancies for $Z=59$ are $\Gamma \approx 5$ eV, and the differences between the three widths may be as large as 2 eV.¹⁶ The measured linewidth in

Fig. 3 is 0.084% in momentum or ~ 80 eV in energy whereas in Fig. 2 it is 0.05% in momentum or ~ 230 eV. Thus we can expect up to $\sim 2\%$ variations in the widths of the "true" shape of the L 57 lines and much smaller differences for the L 293 lines. The increase in instrumental linewidth Δp with p (effect *b*) going from the L_I to L_{III} lines is 0.9% in Fig. 3 and only 0.15% in Fig. 2. This is compensated in part by the decrease in fractional width due to energy losses (effect *c*).

Bearing in mind that no two conversion line shapes are identical, one should evaluate line intensities from the total areas,

$$A = \int_0^\infty \frac{N(p)}{p} dp, \quad (2)$$

where $N(p)$ is the net observed counting rate from the line at momentum setting p . In practice we have evaluated line areas using the relation

$$A = (p_0)^{-1} \sum_{p_l}^{p_u} N(p) \Delta p, \quad (3)$$

where Δp is the step size and p_0 is the momentum of the line peak. The upper and lower limits, p_u and p_l , were chosen to be the points at which $N(p)$ falls to 1% of $N(p_0)$, as indicated by the fitted line shapes on the semilogarithmic plot. In order to carry through statistical errors and minimize any systematic error from the assumption of a common line shape, we first sum

¹⁶ G. Kaye, Nucl. Phys. 68, 529 (1965).

TABLE I. Internal conversion line intensity ratios.

Nucleus	E_γ (keV)	$K/\Sigma L$	$L_I : L_{II} : L_{III}$	%E2	References
^{148}Pr	57.37 ± 0.05	...	1000 : 91.0 ± 1.7 : 27.2 ± 0.7	0.15 ± 0.03	This work
		...	1000 : 80 ± 7 : 29.4 ± 5.3	<0.3	4
^{148}Pr	293.3 ± 0.1	6.04 ± 0.13	1000 : 177 ± 10 : 114 ± 6	37 ± 4	This work
		...	1000 : 192 ± 26 : 77 ± 24	34 ± 16	4
		6.1 ± 0.6	1
^{141}Pr	145.43 ± 0.02	...	1000 : 78.0 ± 1.1 : 19.68 ± 0.23	0.42 ± 0.08	This work
		...	1000 : 81 ± 4 : 17.2 ± 2.5	0.4 ± 0.3	23

the observed counts C over the resolved portions of the peaks, $S = \sum C(p)$, and subtract the sum of the corresponding background counts for the same region N_{bgd} . The summation is then extended to the chosen upper and lower limits by summing the necessary tail area contributions T_i from the graphical plot and adding or subtracting as required. Making the arbitrary but safe assumption that the areas of these tail portions have uncertainties of 10%, we deduce a fractional error to be assigned to the line area from the relation

$$\sigma = \frac{\Delta p}{p_0 A} [S + N_{\text{bgd}} + (0.1 \sum T_i)^2]^{1/2}. \quad (4)$$

The relative L -shell conversion line intensities for the 57- and 293-keV transitions obtained from our data are given in Table I. The transition multiplicities have been determined from the comparison of the measured L -line intensity ratios with theoretical conversion coefficient ratios evaluated from the tables of Sliv and Band. These comparisons are given in Fig. 4. The multipolarity admixtures inferred from the L_{II}/L_I and

L_{III}/L_I ratios are seen to be consistent with one another in both cases. The multipolarity admixtures for the respective transitions which we have adopted from these comparisons are given in Table I.

IV. MEASUREMENT AND DISCUSSION OF $\alpha_K(57.37)$

In our first two measurements of $\alpha_K(57.37)$, a weak source of ^{148}Ce was placed between the 30-cm³ Ge(Li) detector and the NaI(Tl) scintillation detector. A single-channel analyzer was set on the cleanly resolved 293-keV γ -ray peak in the Ge(Li) detector spectrum. A coincidence between this and any pulse from the NaI(Tl) detector gated the pulse-height spectrum from the NaI(Tl) counter to the multichannel analyzer. The resultant spectrum was resolved into the 57-keV and K x-ray components using, as an aid, the shape of a singles 60-keV γ -ray peak obtained with a source of ^{241}Am . To obtain the conversion coefficient from the ratio of the K x ray to 57-keV peak areas we have corrected for (a) the effect of the 293- and 57-keV γ - γ correlation assuming $A_2 = 0.139$ and taking account of the known counter solid angles, (b) the K fluorescence yield in Pr, assumed to be 0.900,¹⁷ (c) the areas of the escape peaks,¹⁷ and (d) the calculated difference between the absorption of x rays and 57-keV γ rays due to the β absorber and NaI light shield. Two similar measurements made in this way gave values for α_K of 6.4 ± 0.7 and 6.2 ± 0.4 .

In these two measurements no allowance was made for a possible contribution to the coincidence spectrum from 293-keV γ ray and bremsstrahlung coincidences. Rather than attempt to determine what effect this contribution might have we have carried out a third experiment designed to reduce this effect. The source was placed between the NaI(Tl) crystal and a plastic phosphor scintillation detector with the Ge(Li) detector at about 90°. A coincidence between β rays ($E > \sim 0.6$ MeV) in the plastic phosphor and 293-keV pulses from the Ge(Li) detector provided the gate pulse for the NaI(Tl) pulse-height spectrum. The ratio of peak areas, after making the corrections noted above, gives the value of

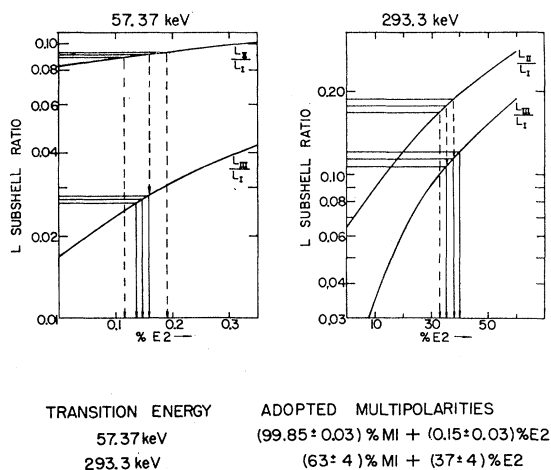
L SUBSHELL RATIOS vs % E2 ADMIXTURE FOR $^{148}\text{Pr}_{84}^{59}$ 

FIG. 4. Deduction of the E2 admixtures in the 57.37- and 293.3-keV transitions in ^{148}Pr by comparing the measured L -subshell intensity ratios with the theoretical ratios of Sliv and Band (Ref. 10).

¹⁷ A. H. Wapstra, G. J. Nijgh, and R. Van Lieshout, *Nuclear Spectroscopy Tables* (North-Holland Publishing Co., Amsterdam, 1959).

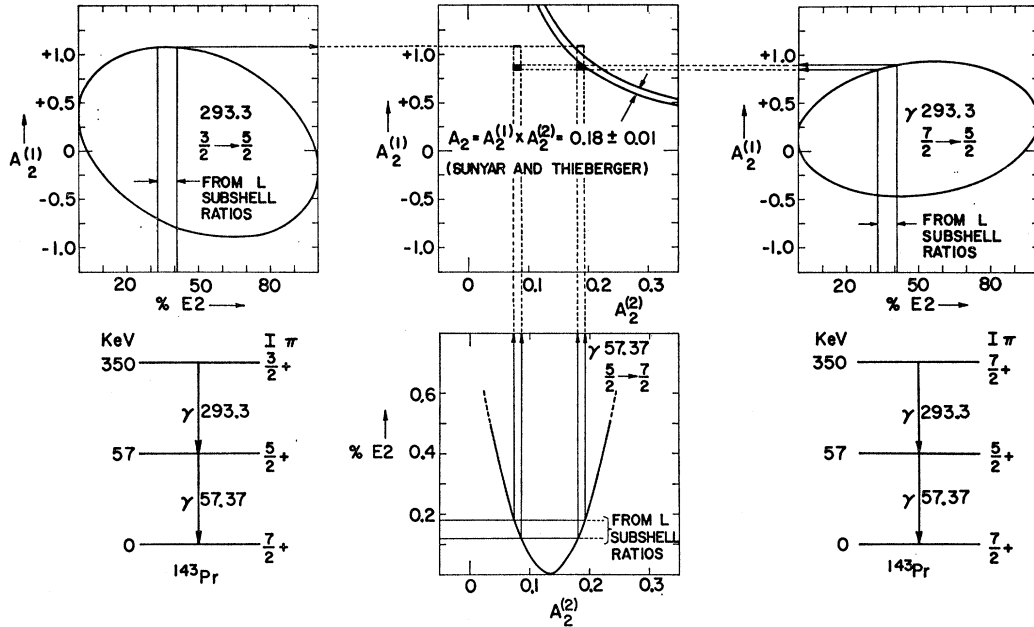


FIG. 5. Graphical analysis of the 293-57-keV γ - γ directional correlation in ^{143}Pr according to the method of Arns and Wiedenbeck (Ref. 19). The predictions for $A_2 = A_2^{(1)}[\gamma 293] \times A_2^{(2)}[\gamma 57.37]$ for two of the possible spin sequences are shown. The $E2$ admixtures determined in this work restrict the theoretical ranges for both $A_2^{(1)}$ and $A_2^{(2)}$. The positive solutions for A_2 are shown as rectangles in the upper central portion. The recent experimental value of $A_2 = 0.18 \pm 0.01$ appears to favor the spin sequence $\frac{7}{2} \rightarrow \frac{5}{2} \rightarrow \frac{7}{2}$ but this possibility is excluded for reasons discussed in the text.

α_K listed in Table II, i.e., $\alpha_K = 5.64 \pm 0.34$, which is consistent with the theoretical value of $\alpha_K = 5.6$.^{9,10}

The experimental values of $\alpha_K(57.37)$ reported to date are compared with the theoretical value in Table II. It is evident from this table that any small discrepancy which may exist between theory and experiment is in the direction of too high an experimental α_K . Church and Weneser¹⁸ have shown theoretically that dynamic nuclear penetration effects in $M1$ transitions make contributions to the K - and L_I -conversion coefficients which are of the same sign and fractional magnitude. The fractional contribution which penetration effects make to the L_{II} -conversion coefficient is somewhat less than that made to the K and L_I coefficients while the contribution made to the L_{III} -conversion coefficient is generally negligibly small. Thus too large an experimental α_K implies an α_{L_I} which is greater than the normal theoretical α_{L_I} and this in turn implies an L_{III}/L_I ratio which is smaller than that predicted by the Sliv and Band theory.¹⁰ It is seen from Fig. 4 that our experimental L_{III}/L_I ratio is instead significantly larger than the theoretical value for pure $M1$ radiation; pure $M1$ character ($< 0.006\%$ $E2$) is required on the $\frac{3}{2} \rightarrow \frac{5}{2} \rightarrow \frac{7}{2}$ spin sequence to account for the 293- and 57-keV γ - γ directional correlation with $A_2 = 0.139 \pm 0.005$.⁸ We conclude that dynamic nuclear penetration effects cannot provide a consistent interpretation for the deviations of our measured L -

subshell ratios from normal pure $M1$ theory. This conclusion was not unexpected; while the 57-keV $M1$ transition is first-forbidden on shell-model arguments ($d_{5/2} \rightarrow g_{7/2}$) its hindrance factor is only ~ 200 .

V. DISCUSSION OF ^{143}Pr RESULTS

The new data presented here yield values for the $E2$ admixtures in 57.37- and 293-keV γ rays which place new and tighter restrictions on the interpretation of the 293- and 57-keV γ - γ angular correlation. The measured value of $\frac{7}{2}$ for the spin of the ground state of ^{143}Pr provides a firm basis for discussing the properties of the 57.37- and 350.7-keV levels.³ The magnetic dipole character of the 57.37-keV transition in principle allows spin values of $\frac{5}{2}$, $\frac{7}{2}$, or $\frac{9}{2}$ for the 57.37-keV level and the magnetic dipole component in the 293.3-keV transition in turn allows spin values of $\frac{3}{2}$, $\frac{5}{2}$, $\frac{7}{2}$, $\frac{9}{2}$, and $\frac{11}{2}$ for the 350.7-keV level. It is of interest to explore which of the nine spin sequences is consistent with the new multipolarity values and the new value of $A_2 = 0.18 \pm 0.01$ obtained by Sunyar and Thieberger from their

TABLE II. Measurements of $\alpha_K(57.37)$.

Year	Reference	Type of experiment	α_K
1956	1	$\gamma - (\gamma + x)$ coinc	5.9 ± 0.6
1963	2	$\gamma - (\gamma + x)$ coinc	6.4 ± 0.6
1966	11	singles	5.9
1966-67	This work	$\beta - \gamma - (\gamma + x)$ coinc	5.64 ± 0.34
	$M1$ theory (Refs. 9, 10)		5.6

¹⁸ E. L. Church and J. Weneser, Ann. Rev. Nucl. Sci. **10**, 193 (1960); Bull. Am. Phys. Soc. **7**, 490 (1962).

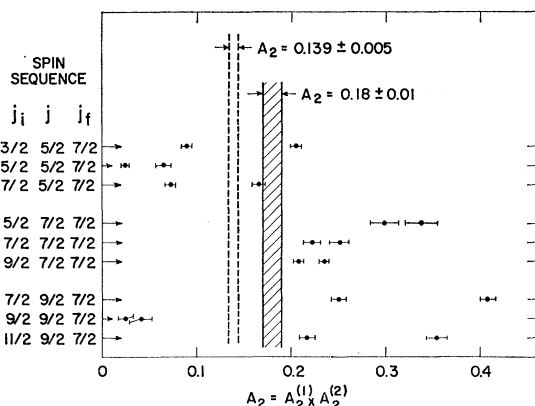


FIG. 6. Plot of A_2 values predicted for the 293- and 57-keV γ - γ directional correlation in ^{143}Pr for nine spin sequences. These 18 values were obtained from graphical analyses of the type shown in Fig. 5 using the multiplicities measured in this work. The experimental value of $A_2 = 0.139 \pm 0.005$ was reported by Sunyar and Thieberger (Ref. 8). In their more recent experiments (Ref. 11) they have measured A_2 versus the time delay in the 57-keV level; extrapolation to zero time gives $A_2 = 0.18 \pm 0.01$.

study of A_2 versus the time delay in the 57.37-keV level which has a lifetime of $T_{1/2} = 4.2$ nsec.⁴ The new value of A_2 comes from an extrapolation to zero time.

Figure 5 shows a graphical analysis for two of the nine spin sequences. The method shown here is that proposed by Arns and Wiedenbeck¹⁹ and is based on the theoretical treatment of Biedenharn and Rose.²⁰ The angular correlation is given by $W(\theta) = 1 + A_2 P_2(\cos\theta) + A_4 P_4(\cos\theta)$, where the coefficient A_2 can be expressed as a product $A_2 = A_2^{(1)} \times A_2^{(2)}$. If the first transition has a fraction Q of quadrupole radiation mixed with a $D = 1 - Q$ dipole fraction then $A_2^{(1)} = a(1 - Q) + b[Q(1 - Q)]^{1/2} + cQ$, where the coefficients a, b, c are functions of the initial and intermediate spins j_i and j and are tabulated.¹⁹ The expression for $A_2^{(2)}$ is similar and one notes that except when $Q = 0$ or 1 there are two values depending on the sign of the interference term $b[Q(1 - Q)]^{1/2}$. In the upper left of Fig. 5 is seen a plot of $A_2^{(1)}$ versus Q for $j_i = \frac{3}{2}$ and $j = \frac{5}{2}$. The measured multipolarity of the 293-keV γ ray ($Q = 0.37 \pm 0.04$) restricts the possible values of $A_2^{(1)}$ to portions of the ellipse between the two vertical lines. The function $A_2^{(2)}$ for the sequence $j = \frac{5}{2}$ (D, Q) $j_f = \frac{7}{2}$ and $Q < 0.006$ is plotted in the lower center of Fig. 5. The measured multipolarity of $\gamma_{57.37}$, $(0.15 \pm 0.03)\%$ $E2$, restricts the possible values of $A_2^{(2)}$ to the regions between the horizontal lines. Thus for the spin sequence $\frac{3}{2}(DQ)\frac{5}{2}(DQ)\frac{7}{2}$ there are four possible products of $A_2^{(1)} \times A_2^{(2)} = A_2$, of which two are positive and two are negative. Since the experimental A_2 is positive we consider only the former, which are shown as the upper two thin rectangular regions in the upper central portion

of Fig. 5. The plot of $A_2^{(1)}$ for $j_i = \frac{7}{2}(DQ)j = \frac{5}{2}$ is shown at the upper right and leads to the two larger shaded rectangles in the upper central box. Only two of these rectangles come close to agreement with the new experimental value of $A_2 = 0.18 \pm 0.01$, i.e., the region between the curved lines. Graphical analyses of the other seven sequences have also been made, and the corresponding 18 positive theoretical values of A_2 have been summarized in Fig. 6.

The spin sequence $\frac{7}{2} \rightarrow \frac{5}{2} \rightarrow \frac{7}{2}$ favored by the above analysis is not supported by the known properties of the β feeds from ^{143}Ce to these three levels. The atomic beam measurement of Maleh²¹ establishes the spin of ^{143}Ce as $\frac{3}{2}$. Intense β feeds to the 57.37-keV level (38%) and to the 350.7-keV level (42%) have $\log ft$ values of 7.7 and 7.3, respectively.¹ Both $\log ft$ values are in the range expected for first-forbidden β decay (spin change of 0 or 1) and Martin *et al.*¹ concluded that their data on all the β -spectrum components were consistent with allowed shapes. However, their data are not sufficiently accurate to exclude the possibility that one of the components might be first-forbidden unique (spin change of 2) having a nonallowed shape. From the histogram plot of $\log ft$'s for unique first-forbidden β transitions given by Gove²² one sees that all well-established cases have $\log ft$ values lying between 7.6 and 9.8. It is therefore most unlikely that the β transition to the 350.7-keV level ($\log ft = 7.3$) is unique; a spin change of 0 or 1 limits the spin of the 350.7-keV level to $j \leq \frac{5}{2}$. Of the nine spin sequences considered in Fig. 6 only three satisfy this new criterion. One can immediately reject the $\frac{5}{2} \rightarrow \frac{5}{2} \rightarrow \frac{7}{2}$ sequence because the experimental A_2 is much greater than the predic-

TABLE III. Summary of results for the 293- and 57-keV γ - γ angular correlation.

Year	Reference	A_2	Quoted spin assignments		
			351 keV	57 keV	Ground
1963	2	0.132(19)	$\frac{3}{2}$	$\frac{7}{2}$	$\frac{5}{2}$ ^a
1963	4	(analysis of above)	$\frac{3}{2}$ or $\frac{7}{2}$	$\frac{5}{2}$	$\frac{7}{2}$ ^b
1963	c	0.132(10)
1964	d	0.133(7)	$\frac{3}{2}$	$\frac{5}{2}$	$\frac{7}{2}$
1964	5	0.106(10)	$\frac{7}{2}$	$\frac{5}{2}$	$\frac{7}{2}$
1965	6	0.123(11)	$\frac{7}{2}$	$\frac{5}{2}$	$\frac{7}{2}$
1965	7	0.112(9)	$\frac{3}{2}$	$\frac{5}{2}$	$\frac{7}{2}$
1966	e	0.125(6)
1966	8	0.139(5)	$\frac{3}{2}$	$\frac{5}{2}$	$\frac{7}{2}$
1966	11	0.180(10)	$\frac{3}{2}$	$\frac{5}{2}$	$\frac{7}{2}$

^a Spin assumed to be 5/2 from systematics.

^b The measured spin of the ground state is 7/2⁽³⁾.

^c E. Bozek, A. Z. Hryniewicz, S. Ogaza, M. Rvbicka, and J. Styczen, Phys. Letters 6, 89 (1963).

^d R. M. Levy, Ph.D. thesis, Lawrence Radiation Laboratory Report No. UCRL-11663, 1964 (unpublished).

^e H. Zmorá, S. Ofer, and M. Rakavy, Nucl. Phys. 89, 225 (1966).

²¹ I. Maleh, Phys. Rev. 138, B766 (1965).

²² N. B. Gove, in *Nuclear Spin-Parity Assignments*, edited by N. B. Gove and R. L. Robinson (Academic Press Inc., New York, 1966), p. 83.

¹⁹ R. G. Arns and M. L. Wiedenbeck, Phys. Rev. 111, 1631 (1958).

²⁰ L. C. Biedenharn and M. E. Rose, Rev. Mod. Phys. 25, 729 (1953).

tions using the known multipolarities. The $\frac{5}{2} \rightarrow \frac{7}{2} \rightarrow \frac{7}{2}$ sequence seems an unlikely choice since it requires (a) that the β feed to the 57.37-keV level ($\log ft = 7.7$) be first-forbidden unique and (b) that there remains a large and as yet undetected attenuation in A_2 . The spin sequence $\frac{3}{2} \rightarrow \frac{5}{2} \rightarrow \frac{7}{2}$ does not require a first-forbidden unique β decay. The value of $A_2 = 0.203 \pm 0.006$ predicted for the spin sequence, $\frac{3}{2} \rightarrow \frac{5}{2} \rightarrow \frac{7}{2}$, is higher than $A_2 = 0.18 \pm 0.01$ by twice the combined errors. The summary of experimental A_2 values listed in Table III shows that large attenuations have been present in all the earlier measurements of this γ - γ correlation. It seems probable to us that the discrepancy between the latest measurement and that predicted for $\frac{3}{2} \rightarrow \frac{5}{2} \rightarrow \frac{7}{2}$ results from attenuation effects which have as yet gone undetected.

Experiments which demonstrate conclusively non-unique shapes for the β -ray components to the 57.37- and 350.7-keV levels would provide the final convincing argument for the choice of a $\frac{3}{2} \rightarrow \frac{5}{2} \rightarrow \frac{7}{2}$ spin sequence.

VI. MULTIPOLARITY OF THE 145.43-keV TRANSITION IN ^{141}Pr

We have remeasured the L -subshell conversion electron intensity ratios of the 145.43-keV transition in ^{141}Pr , at a momentum resolution of 0.05%. The data

were accumulated using a multistrip source and the rapid-scan technique described above. Our results for the L -subshell ratios of this transition are $L_I/L_{II} = 12.82 \pm 0.18$ and $L_I/L_{III} = 50.8 \pm 0.6$. The inverse ratios are summarized in Table I. Comparison with the ratios of the theoretical internal conversion coefficients of Sliv and Band¹⁰ shows that this transition is dominantly $M1$ with an $E2$ admixture of $(0.42 \pm 0.06)\%$. This result is consistent with the $E2$ admixture of $(0.4 \pm 0.3)\%$ $E2$ reported by Geiger *et al.*²³ The higher accuracy realized in the present work results from the use of the multistrip source and rapid-scan techniques.

ACKNOWLEDGMENTS

It is a pleasure to thank W. L. Perry and Mrs. J. S. Merritt for their assistance in source preparation and R. B. Walker for his technical help with the multistrip source and rapid scan techniques. We are grateful to Allan Hewitt for his fabrication of the multistrip source assembly and for his significant contributions to its mechanical design.

One of us (W.G.) has held a National Research Council of Canada Postdoctoral Fellowship during the period of this work.

²³ J. S. Geiger, R. L. Graham, I. Bergstrom, and F. Brown, Nucl. Phys. 68, 352 (1965).